INFN

ISTITUTO NAZIONALE DI FISICA NUCLEARE

Sezione di Milano

INFN/20-18-MI
24 Novembre 2020

EVALUATION OF THE SHIEDLING IN THE BUNKER FOR THE SUPERCONDUCTING CAVITY TEST AT LASA

Michele Bertucci, Francesco Broggi, Paolo Michelato

[1)]*INFN-Sezione di Milano, Dip. Scienze Fisiche-LASA Via F.lli Cervi 201 20054 Segrate (Milano), Italy*

Abstract

In the LASA (Laboratorio Acceleratori e Superconduttività Applicata) laboratory of the Milan section of INFN (Istituto Nazionale di Fisica Nucleare) a facility for testing superconducting cavities is operating. The possibility to operate with a generation of radiation up to 10 MeV and more requires a careful evaluation of the shielding efficiency of the existing bunker

The calculation was performed with the FLUKA code, the whole cryostat, bunker and ceiling of the building was taken into account. Two hypothesis for the radiation source have been adopted to carry out the calculations: the very conservative hypothesis of 10 MeV electron pencil beam, and the second hypothesis (maybe more realistic) of an isotropic 10 MeV electron source. In the less conservative hypothesis a safe operation is guarantee by the foreseen shielding.

The simulations show that even in the most conservative hypothesis a negligible amount of photons can exit the bunker, without interaction with the simulated detectors.

In the future, at the starting of the tests in the upgraded configuration, direct measurements will be used to definitely check the shielding adopted.

PACS.: 28.41.Te

Published by ***SIS–Pubblicazioni***
Laboratori Nazionali di Frascati

Work performed in the frame of the MC-INFN, and ESS activity

1 INTRODUCTION

At the LASA (Laboratorio Acceleratori e Superconduttività Applicata) of the Milan section of the INFN (Istituto Nazionale di Fisica Nucleare) a test facility for superconducting cavities is operating (see fig.1).

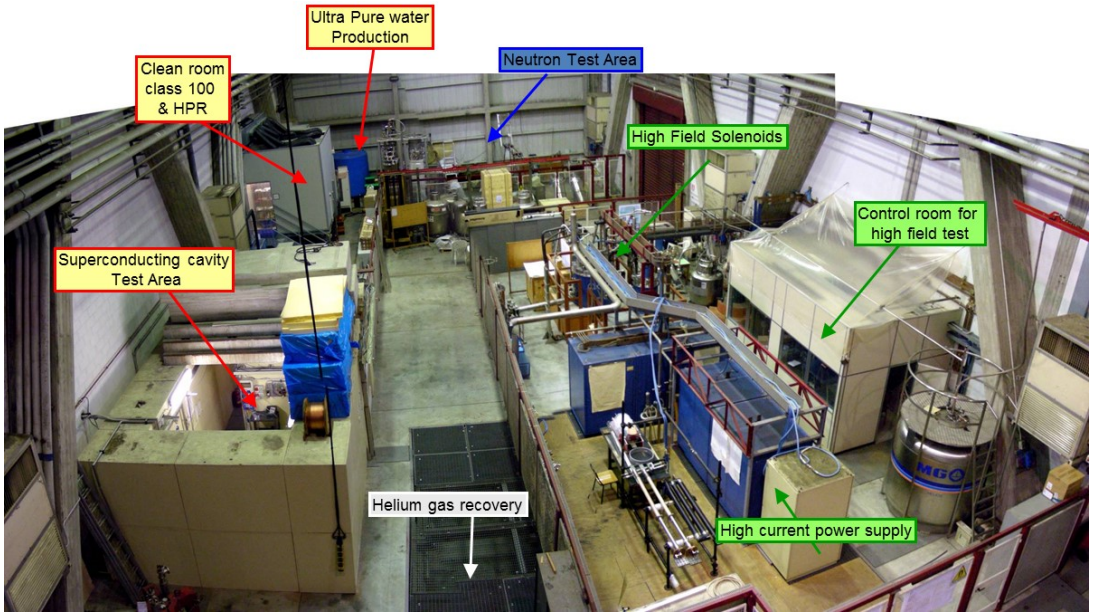

Figure 1: View of the LASA experimental area. The RF bunker is at the bottom left (concrete roof removed).

The cavity operation can induce the production of X-rays, through the mechanism of "field emission": electrons are extracted from cavity surface by the effect of the time-varying electromagnetic field excited in the cavity. The same field accelerates the electrons until they impact against the cavity surface, eventually producing Bremsstrahlung X-ray radiation.

The tests performed in the past show moderate levels of radiation outside the cryostat and absolutely negligible levels of radiation outside the bunker[1,2]. In the future, it is planned to improve the Vertical Test Facility in order to test cavity with bigger accelerating gradients and Q-values. This scenario requires an accurate evaluation of the radiation levels in several points of interest inside the lab. In order to reconstruct the most pessimistic picture, we assume what follows:

- One expects that, due to higher accelerating fields, an X-ray energy up to 10 MeV can now be achieved. Such number can be assumed as a conservative estimation of electron impact energy
- The cryogenic limit of operation is 50W. We assume the limit case where, on average, all this power is transferred inside the electron current.
- The corresponding current is obtained as I=P/V=50W/10MV=5 μA and corresponds to $N=I/e^{-}=5\ \mu A/(1.6 \times 10^{-19}\ C)=3 \times 10^{13}$ e/sec.

The evaluation has been performed with the FLUKA code [3,4,5]. The results obtained by FLUKA, which are normalized on the total number of primary particles, can be then scaled on the real case assuming $3x10^{13}$ primary particles per second.

The calculations have been done by assuming two hypothesis:

- The ultra-conservative one: by which the dark emission is simulated by a 10 MeV pencil beam focused to the closing flange, pointing towards the cryostat cover.
- The most-probable hypothesis: by which the dark current is described by an isotropic 10 MeV electron source.

The first one is ultra-conservative because it implies that the emitted electron must be in phase with the RF and undergo to the "right" accelerating field all along the cavity.

The second one is a more realistic assumption but with keep the conservative statement of the 10 MeV electron energy.

2 THE FLUKA MODEL

The cryostat, housing the cavity under test, consists of a stainless steel cylinder 4.45 cm thick and about 470 cm long. Around it there is a 3 cm mu-metal shield 410 cm long (there is no need to shield the top part).

Inside the cryostat there is the cavity under test, it is closed on top with a stainless steel flange 2.1 cm thick.

Over the cavity there is a thermal shield composed by 4 copper disks.

In fig. 2 the cavity and supports are shown; everything is inserted into the cryostat.

The cryostat is inserted in a hole in the floor so the closing flange of the cryostat is at about 1 m above the floor level while the closing flange of the cavity is about 2 m under the floor level.

The bunker walls consist of Portland concrete 1 m thick. The ceiling of the bunker is of Portland concrete 50 cm thick and 75 cm thick (see Fig. 3).

For some runs the building roof of concrete (20 cm thick) has been neglected to evaluate a possible skyshine effect (see Appendix).

The possibility of activating some cryostat materials, has been evaluated by simulating a test run with a current of 10^{13} electrons/sec for 12 hours of continuous powering of the cavity.

Some detectors have been considered, in order to evaluate the amount of a possible dose in the regions around the bunker. They are located at about 1.5 m away from the bunker wall, one on the side facing the magnet test area, one facing the building entering door and one in the bunker access corridor and another detector right on the bunker ceiling on axis with the cryostat; for same runs a detector on axis with the cryostat at about 1.8 m from the floor (so it is inside the bunker) has been considered.

Figure 2: View of the niobium cavity (violet) with the four copper disks and the support system. Everything is enclosed into the cryostat.

The radiation source due to the field-emitted electrons from the cavity surface is (very conservatively) schematized as a monochromatic pencil beam of 10 MeV electrons 0.5 mm radius starting from the bottom of the cryostat, upward directed, hitting the closing flange of the vacuum chamber.

The transport cut-offs for electrons and photons are set at 10 keV, and the photonuclear reactions are taken into account.

One case has been studied by simulating the source as an isotropic point electron source located at 2 m under the floor level, inside the vacuum chamber.

Routines to describe the field emission from high voltage radiofrequency cavities have been developed[6] but for this preliminary study we do not think necessary to use them.

All the simulations have been obtained with 10 runs with different random seeds with 10^7 primaries each.

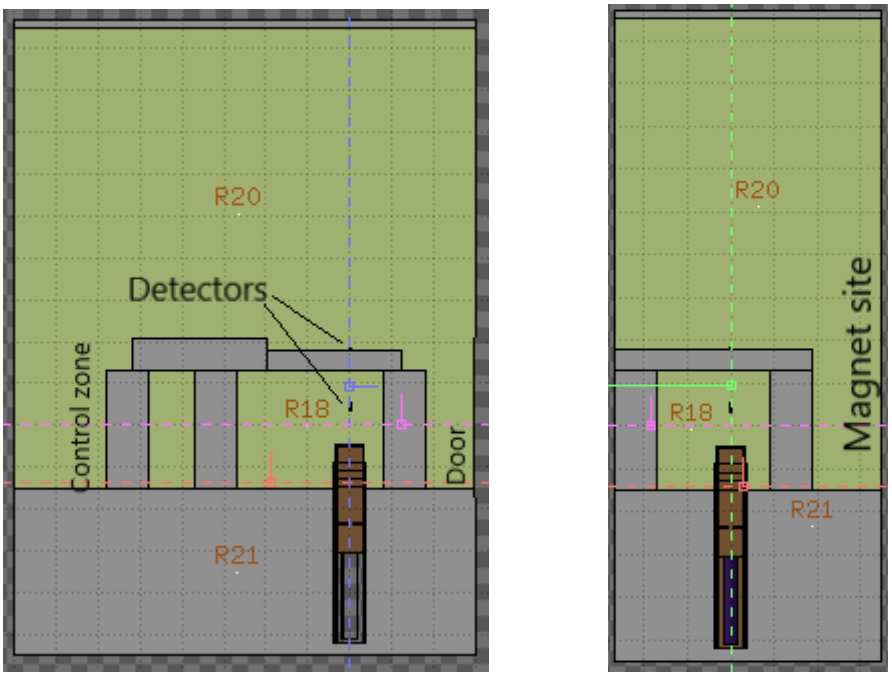

(a) (b)

Figure 3: Side view of the bunker from the building wall (a) (i.e. from the left side of fig.1) and (b) from the building door (i.e. from the bottom of fig.1). The detector on axis with the cryostat are visible (one inside the bunker the other just on the concrete ceiling).

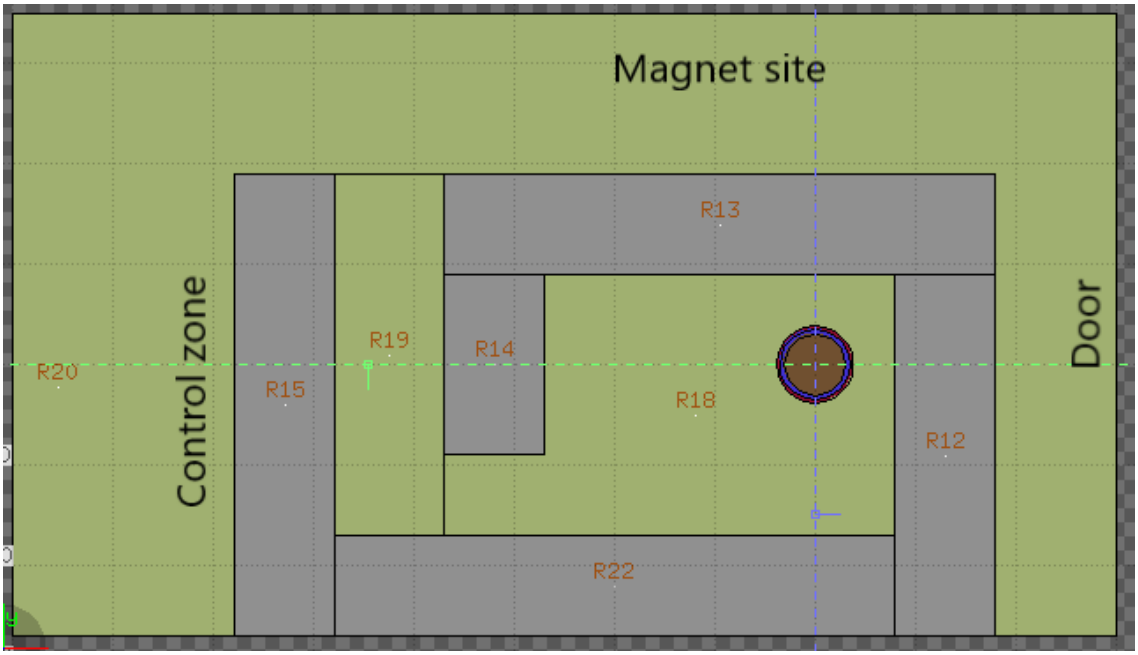

Figure 4: Bunker and cryostat top view.

3 FLUKA SIMULATION RESULTS

In fig, 5, 6 and 7 the fluencies of the photons, electrons and positrons and the corresponding fluencies at the “human” level, i.e. between the floor level and 2.5 m are shown.

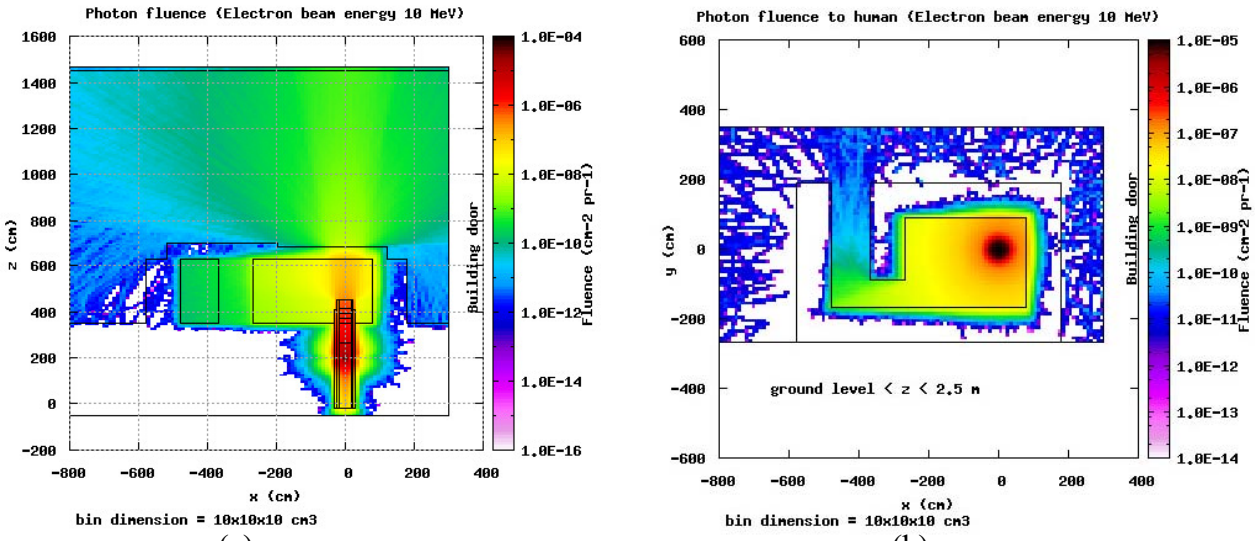

(a) (b)

Figure 5: (a) View of the photon fluence and (b) top view of the of the photon fluence between the floor level and 2.5 m (human window).

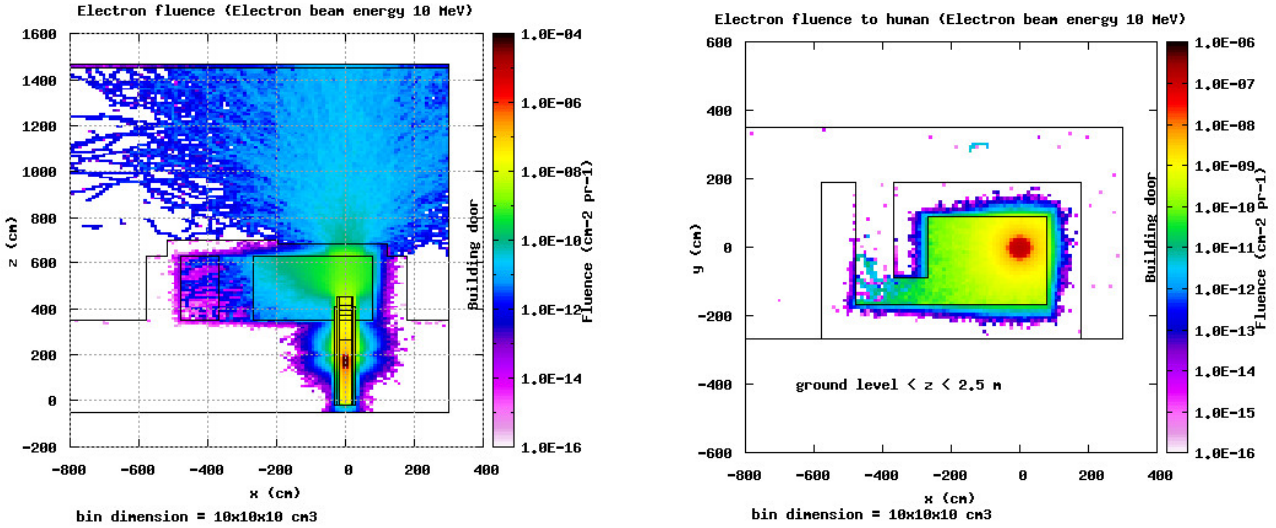

(a) (b)

Figure 6: (a) View of the electron fluence and (b) top view of the of the electron fluence

and

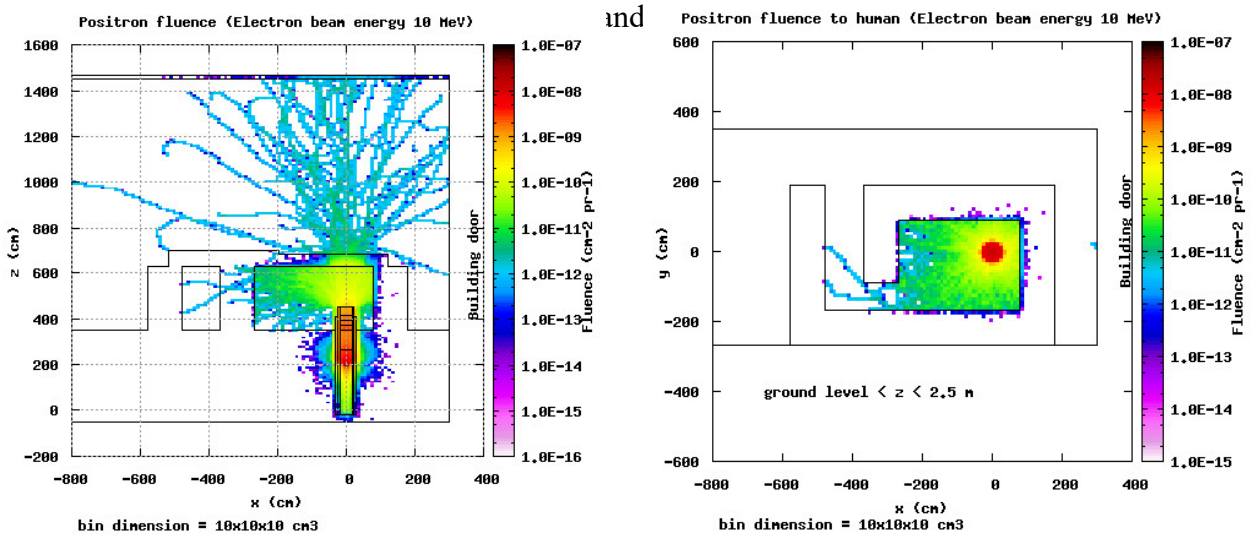

(a) (b)

Figure 7: (a) View of the positron fluence and (b) top view of the of the positron fluence between the floor level and 2.5 m (human window).

3.1 Fluencies toward the building door

In the following figures the fluencies of the photons, of the electrons and positrons in the air just outside the walls of the bunker facing the building door, up to 3 m from them, are shown. They are indicated with “Door”, meaning the space toward the building door (toward the bottom of fig.1), “Magnets”, meaning the space toward the magnet test area (right part of fig.1) and “Control” i.e. toward the RF and cryostat control rack (top part of fig.1).

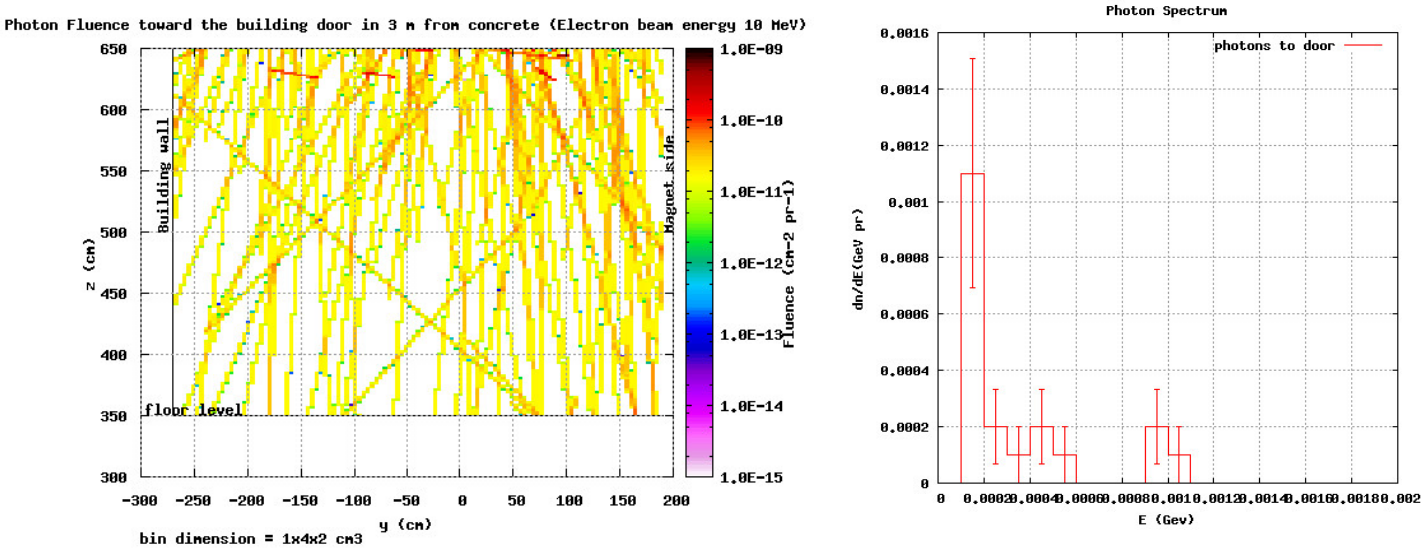

(a) (b)

Figure 8: (a) Photon fluence in 3 m outside the bunker wall toward the building door between ground level and 3 m height. (b) Spectrum of the photons exiting the bunker wall toward the building door (the data are meaningless, see text for details).

According to the spectrum the photon exiting the bunker wall are $2x10^{-7}$ +/- 18% photons/primary. The FLUKA simulation has been carried out over 10 runs with different random seeds with 10^7 primaries each. It follows that the spectrum is obtained with only twenty photons, so it statistically irrelevant.

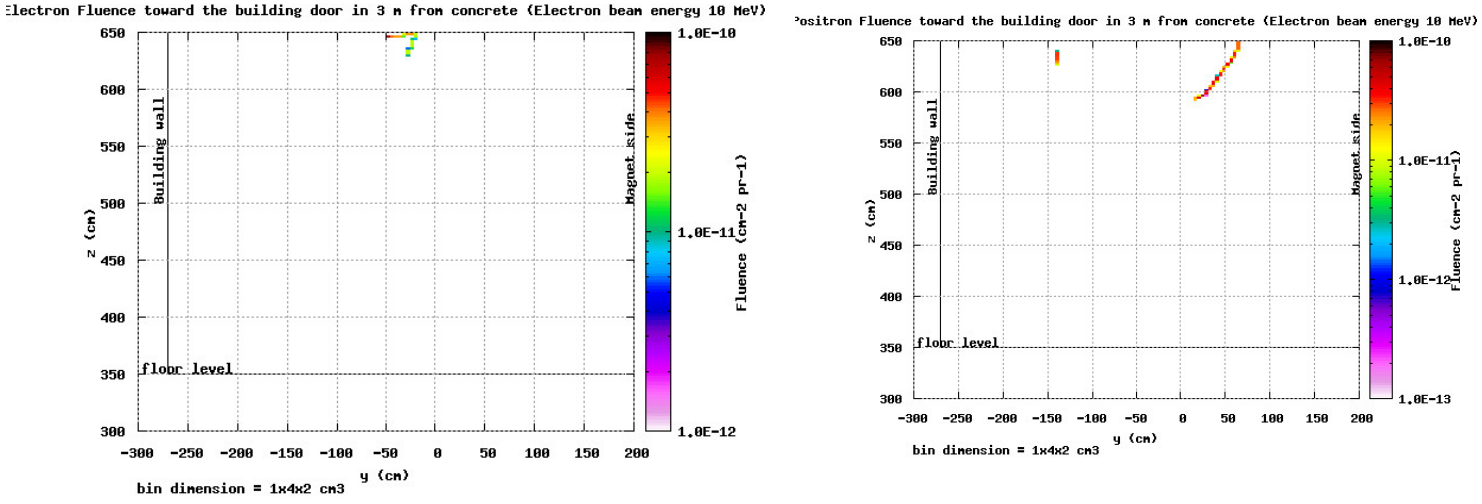

(a) (b)

Figure 9: Electron fluence (a) and positron fluence (b) in 2.5 m outside the bunker wall toward the building door between ground level and 2.5 m height.

No spectra for electron and positrons are shown because fluence from the wall to the air is null everywhere. The (very few) electrons and positrons shown are probably due to a skyshine effect.

3.2 Fluencies toward the magnet side

In the following figures the fluencies of the photons and of the electrons in the air just outside the walls of the bunker facing the magnet test area, up to 3 m from them are shown.

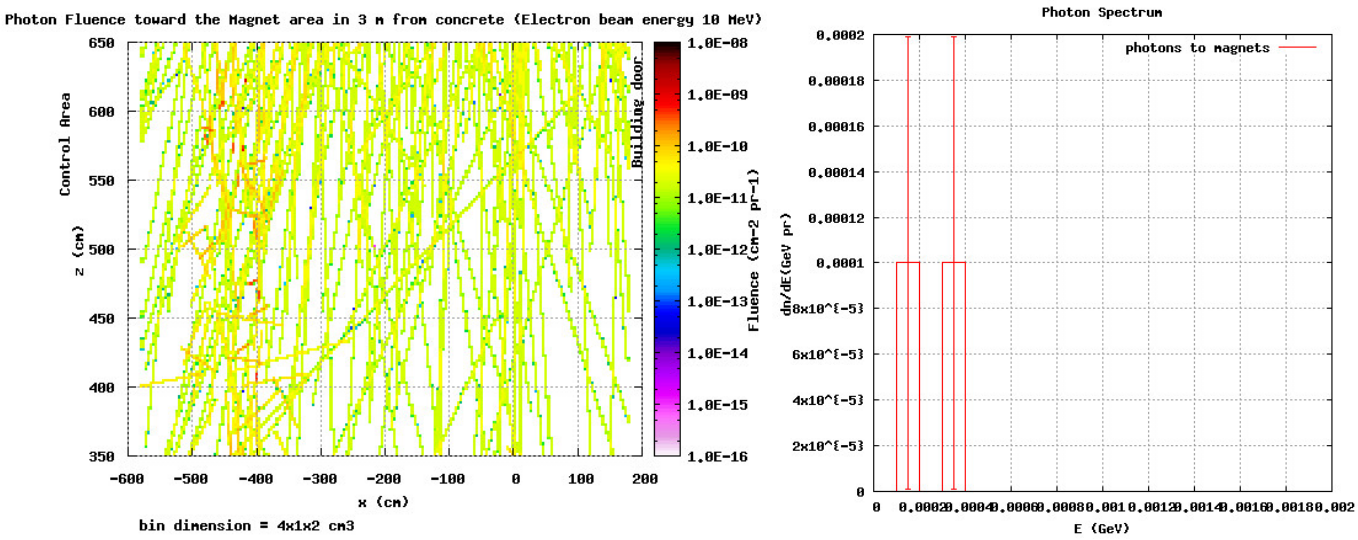

(a) (b)

Figure 10: (a) Photon fluence in 3 m outside the bunker wall toward the magnet test area between ground level and 3 m height. (b) Spectrum of the photons exiting the bunker wall toward the magnet test area (the data are meaningless, see text for details).

As we can see from the spectrum, very few photons come directly from the bunker wall, the others are generated outside. In this region there are no positrons

According to the spectrum the photon exiting the bunker wall are $2x10^{-8}$ +/- 66% photons/primary. The FLUKA simulation has been carried out over 10 runs with different random seeds with 10^7 primaries each. It follows that the spectrum is obtained with only two photons, so it is statistically irrelevant.

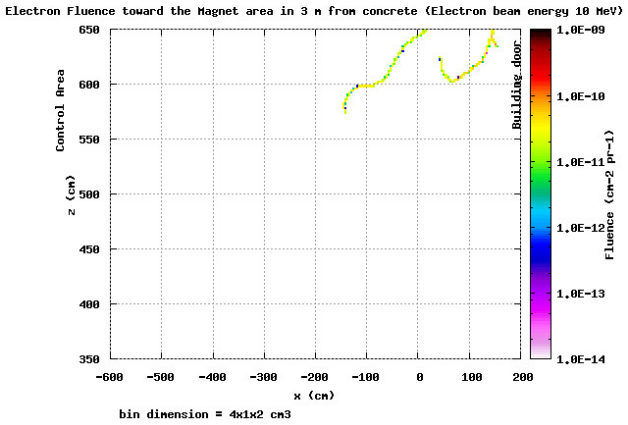

Figure 11: (a) Electron fluence in 3 m outside the bunker wall toward the magnet test area between ground level and 2.5 m height. No electrons come directly from the bunker wall.

3.3 Fluencies toward the control area

In the following figures the fluencies of photons electrons and positrons toward the control area between the bunker wall and 2.5 m away from it in the “human” region (i.e. between the floor level and 2.5 m height) are shown.

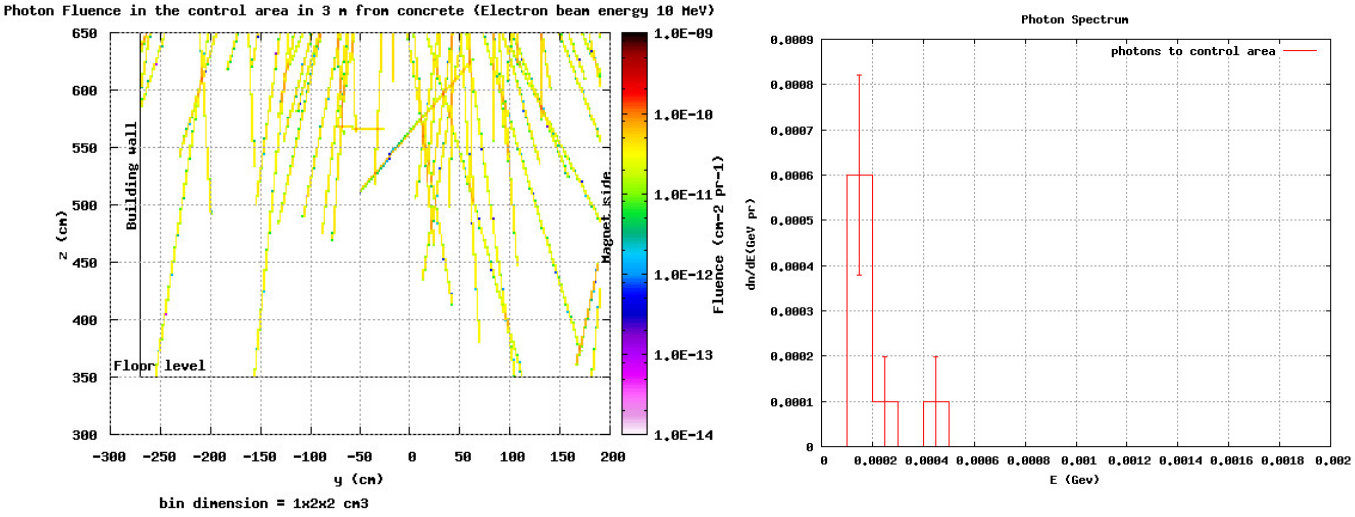

(a) (b)

Figure 12: (a) Photon fluence in 3 m outside the bunker wall toward the control area between ground level and 3 m height. (b) Spectrum of the photons exiting the bunker wall toward the control area (the data are meaningless, see text for details).

According to the spectrum the photon exiting the bunker wall are 8×10^{-8} +/- 25% photons/primary. The FLUKA simulation has been carried out over 10 runs with different random seeds with 10^7 primaries each. It follows that the spectrum is obtained with only eight photons, so it is statistically irrelevant.

3.4 Neutrons and activation

In Fig. 13 the neutron fluence in shown. As we can see there are only few neutrons produced inside the cryostat (and well under the floor level) so there is not any concern about neutron absorption by people inside the building area.

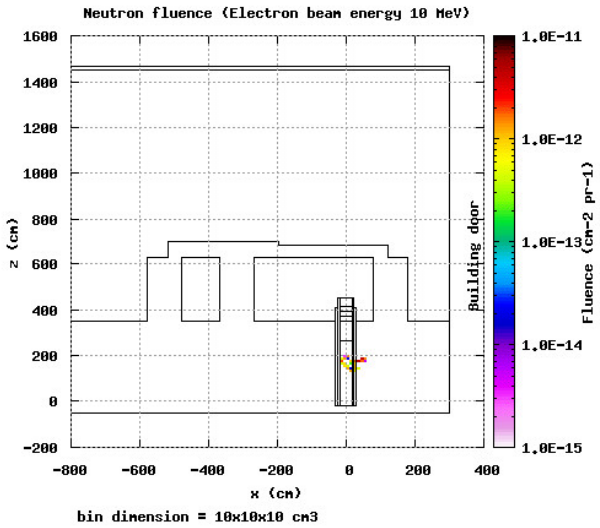

Figure 13: Neutron fluence. Very few neutrons are produced inside the cryostat and under the floor level (located at z=350 cm).

Concerning the activation of the cryostat material in this case only the mu-metal surrounding the cryostat shows an activation of ^{59}Ni, but the value of the activated nuclei ($1x10^{-8}$ nuclei/primary) is negligible and it does not represent any concern.

4 ISOTROPIC SOURCE

Another case has been investigated, by considering the primary electron beam as isotropic, located near the upper vacuum flange of the cavity, instead of the pencil beam considered so far.

The following plots show, as the one in Fig. 14, 15 and 16, the fluencies of the photons, for the electrons and of the positrons.

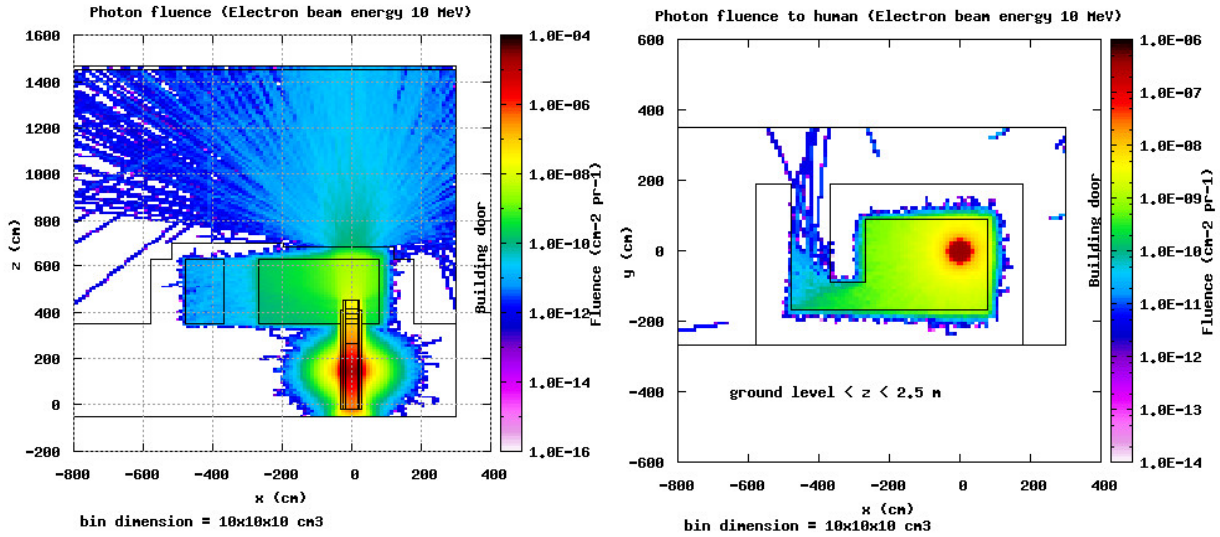

(a) (b)

Figure 14: (a) View of the photon fluence and (b) top view of the of the photon fluence between the floor level and 2.5 m (human window) with an isotropic electron source.

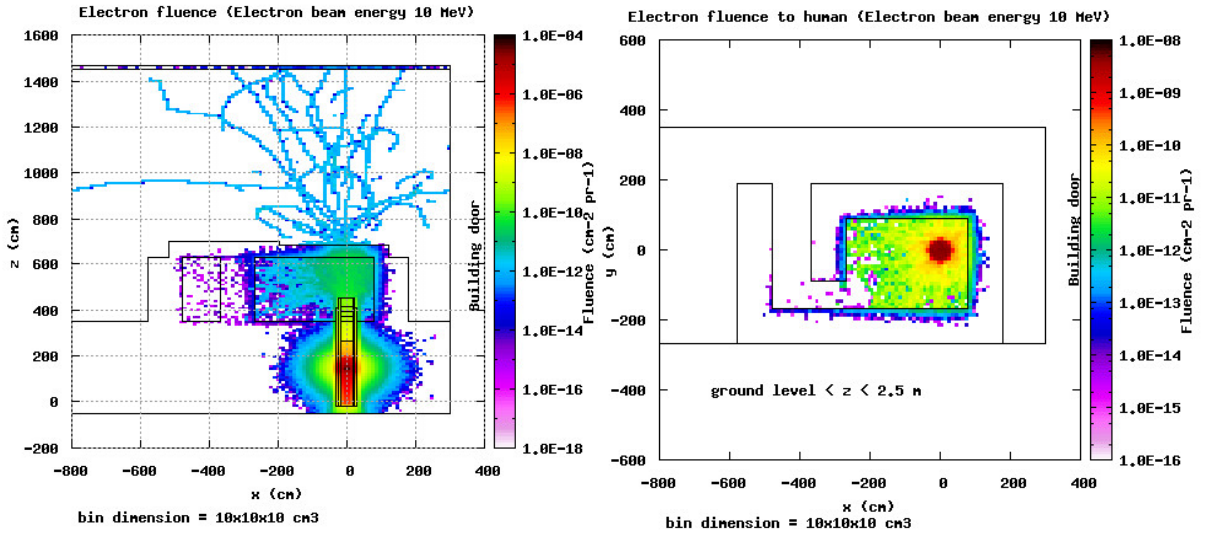

(a) (b)

Figure 15: (a) View of the photon fluence and (b) top view of the of the photon fluence

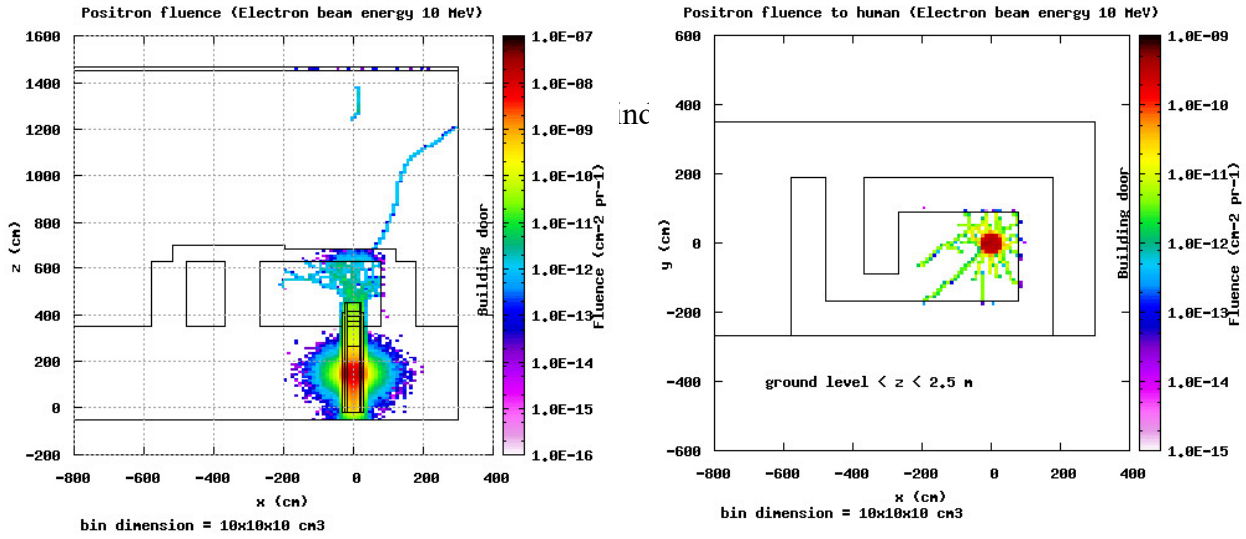

(a) (b)

Figure 16: (a) View of the photon fluence and (b) top view of the of the photon fluence between the floor level and 2.5 m (human window) with an isotropic electron source

As we can see the fluencies in the area external to the bunker is much less the case with the pencil beam, only some (very few) photons are present toward the building door and toward the control area are less than the previous case, so the plots are not reported.

4.1 Neutrons and activation

In fig. 17 the neutron fluence is shown. As we can see little more neutrons are produced in this case with respect to the case of pencil beam (see fig. 13). As in the previous case the neutrons are produced well under the floor level so they do not represent any concern for people irradiation.

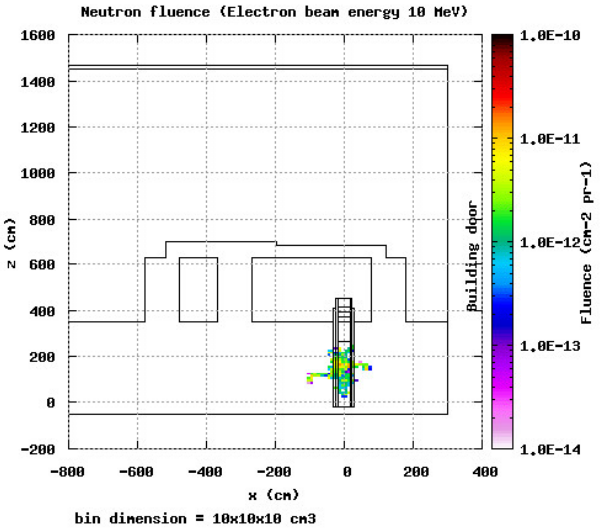

Figure 17: Neutron fluence. Very few neutrons are produced inside the cryostat and under the floor level (z=350 cm).

Concerning the activation of the cryostat material, in this case only the mu-metal surrounding the cryostat shows an activation of ^{59}Ni, ^{63}Ni, ^{64}Cu but the values of the activated nuclei ($1x10^{-8}$ nuclei/primary for ^{63}Ni, ^{64}Cu and $3x10^{-8}$ nuclei/primary for ^{59}Ni) are negligible and they do not represent any concern.

5 CALCULATION REFINEMENTS

Considering the fact that the detectors do not read any energy deposition or dose, because of the small detector dimensions considered (2x2x2 cm^3), we decided to simulate the energy deposited in a human depending on his position in the building outside the bunker.

We defined a sort of human equivalent volume (55x55x200 cm^{3}of water) and we put an array of this "humanoids" at 1m from the bunker wall all around it, as shown in fig.18.

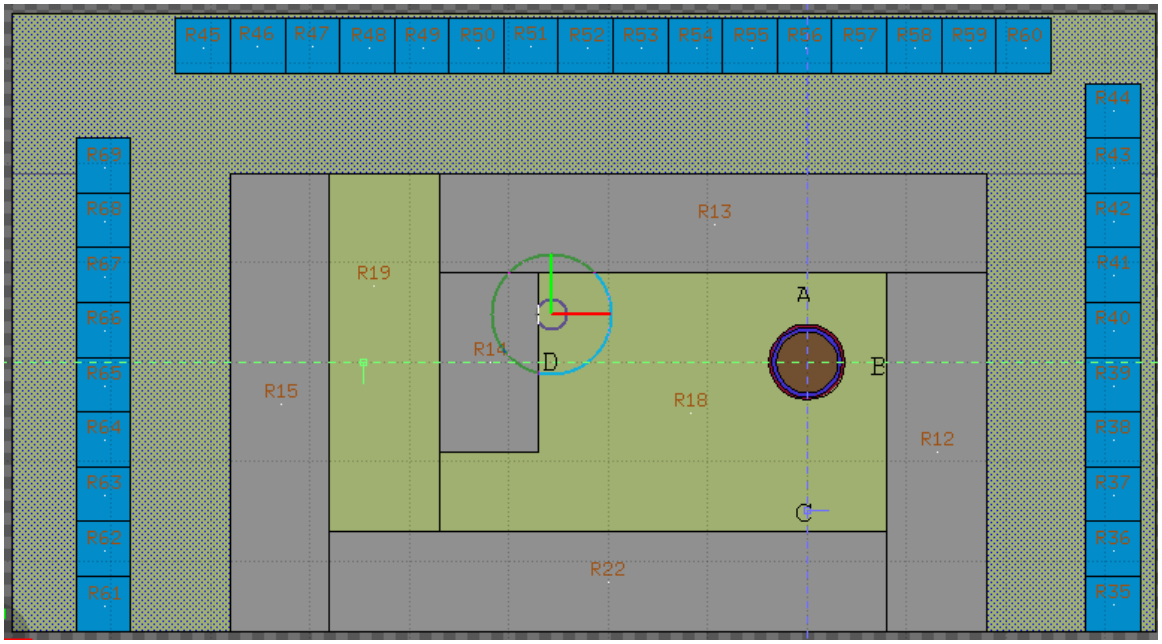

Figure 18: Top view of the "Humanoid" volume all around the bunker; the region number is reported in order to better understand their location and the plot in fig. 19, fig. 20 and fig. 21. The detectors "A", "B", "C", and "D" are shown (see section 5.6)

In addition, in order to increase the shielding and reduce the skyshine effect, we put an iron cylinder (1 m diameter, 20 cm thick) on axis with the cryostat, just above the concrete ceiling of the bunker. According to a first estimation, this iron screen is expected to reduce the intensity of a 10 MeV X-ray beam by a factor 10^2.

In the following figures and tables the results of the simulations with and without the irons shield are shown.

5.1 Energy deposition in the “Humanoid” and Effect of the Iron shield

In the following figures the energy deposition in the “humanoid” regions both with and without the iron shield is shown.

As expected the energy deposed in the considered regions is lower when the iron shield is present, but for region 65 (see Fig. 21), where the energy deposition is slightly higher with the iron shield (gray column) respect to the case without it, this fact may be due to a statistical fluctuation, and being the values so low it can be neglected.

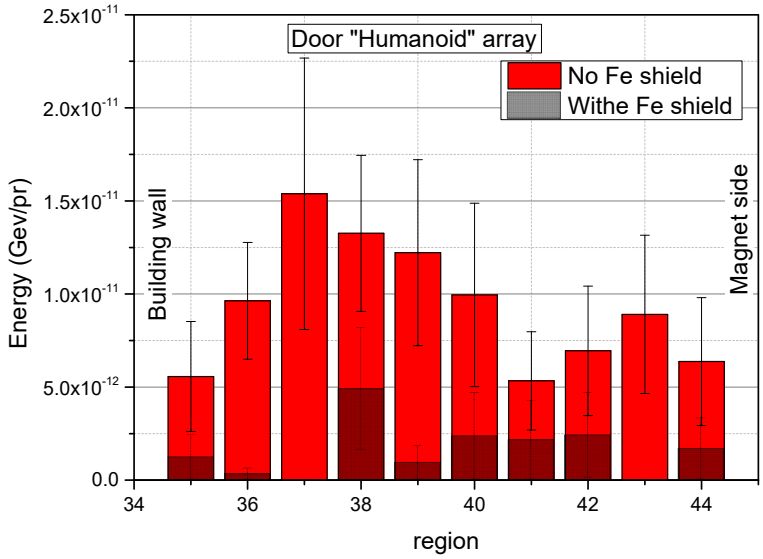

Figure 19: Energy deposition in the “humanoid” region 1 m away from the bunker wall toward the building door

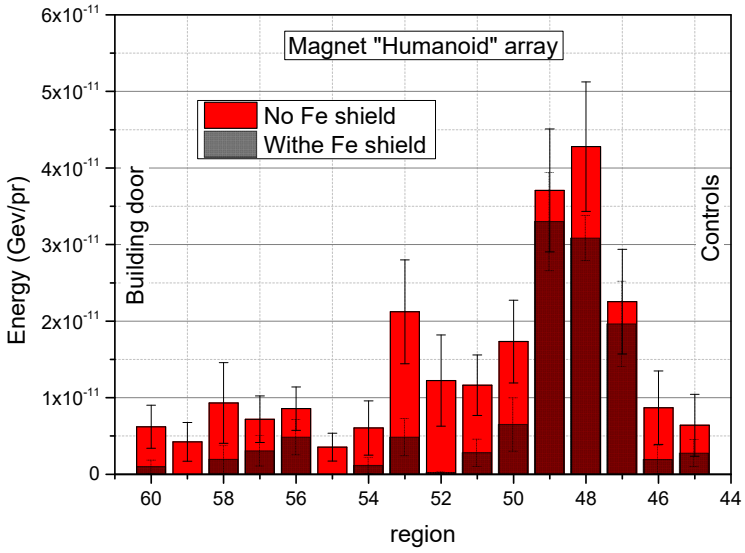

Figure 20: Energy deposition in the “humanoid” region 1 m away from the bunker wall toward magnet area.

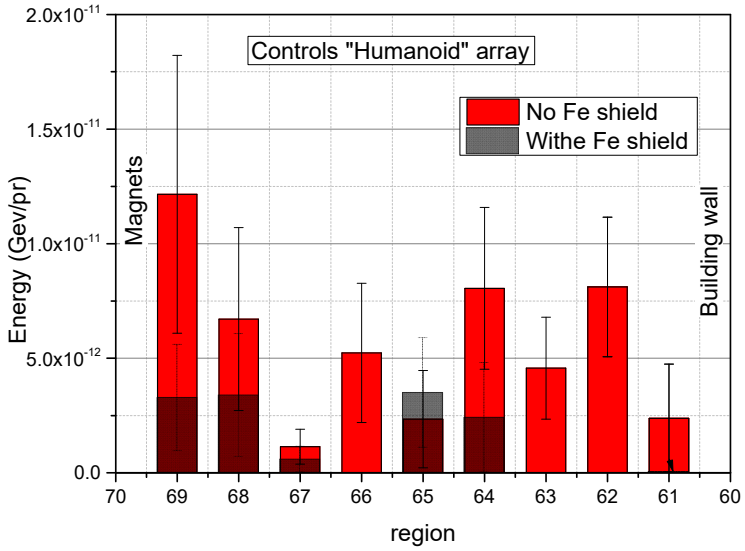

Figure 21: Energy deposition in the “humanoid” region 1 m away from the bunker wall toward the controls area.

The following tables summarize the energy deposition in all the “humanoid” regions together with the error.

The order of the regions is as seen by facing the bunker from left to right (see fig.18)

Table 1: Energy deposition in the "humanoid" regions outside the bunker (see text for details)

		With Iron Shield		Without Iron Shield	
	Region	**Energy (GeV/pr)**	**Error (%)**	**Energy (GeV/pr)**	**Error (%)**
DOOR	35	1.20E-12	99.0	5.57E-12	53.0
	36	2.97E-13	99.0	9.63E-12	32.6
	37	0.00E+00	=	1.54E-11	47.4
	38	4.87E-12	67.5	1.33E-11	31.6
	39	9.00E-13	99.0	1.22E-11	40.9
	40	2.33E-12	99.0	9.95E-12	49.5
	41	2.12E-12	99.0	5.33E-12	49.5
	42	2.38E-12	95.5	6.95E-12	50.1
	43	0.00E+00	=	8.91E-12	47.8
	44	1.65E-12	99.0	6.37E-12	53.9
MAGNETS	60	8.66E-13	99.0	6.21E-12	45.3
	59	0.00E+00	=	4.24E-12	59.8
	58	1.82E-12	99.0	9.31E-12	56.5
	57	2.94E-12	67.5	7.19E-12	42.3
	56	4.74E-12	49.0	8.57E-12	33.0
	55	0.00E+00	=	3.55E-12	51.2
	54	1.02E-12	99.0	6.05E-12	58.6
	53	4.74E-12	51.6	2.12E-11	32.0
	52	8.70E-14	99.0	1.22E-11	48.7
	51	2.69E-12	66.7	1.16E-11	33.9
	50	6.39E-12	54.5	1.73E-11	31.1
	49	3.29E-11	19.5	3.71E-11	21.7
	48	3.08E-11	95.4	4.28E-11	19.8
	47	1.95E-11	28.6	2.26E-11	30.3
	46	1.80E-12	99.0	8.69E-12	55.1
	45	2.64E-12	67.1	6.40E-12	63.1
CONTROL	69	3.25E-12	71.5	1.22E-11	49.9
	68	3.37E-12	79.6	6.71E-12	59.4
	67	5.63E-13	99.0	1.14E-12	66.7
	66	0.00E+00	=	5.24E-12	58.0
	65	3.47E-12	68.9	2.34E-12	90.7
	64	2.39E-12	99.0	8.05E-12	43.8
	63	0.00E+00	=	4.57E-12	48.6
	62	0.00E+00	=	8.11E-12	37.5
	61	5.58E-15	99.0	2.38E-12	99.7

As we can see the error is very high, meaning that the energy deposition values are very low. An error of 99% mean that the energy deposition reported occurs only in one of the 10 different runs of the simulation., so it can be considered as a statistics fluctuation instead of an actual energy deposition.

If we take the maximum value of 3.2910^{-11} GeV occurring in region 49 (the one facing the access corridor) and we suppose a primary intensity of 3E13 primary electrons per second we obtain an energy deposition of in the volume of the "humanoid" (0.605 m^3) 9.610^{-7} J/(kg h), i.e. 0.96 μGy/h.

5.2 Effect of the Iron shield

In the following figures the fluencies of photons, electrons and positrons with the cylinder iron shield are shown, to be compared with the first plots of fig, 5,6 and 7. The shielding effect of the iron and the reduction of the fluencies around the bunker is evident.

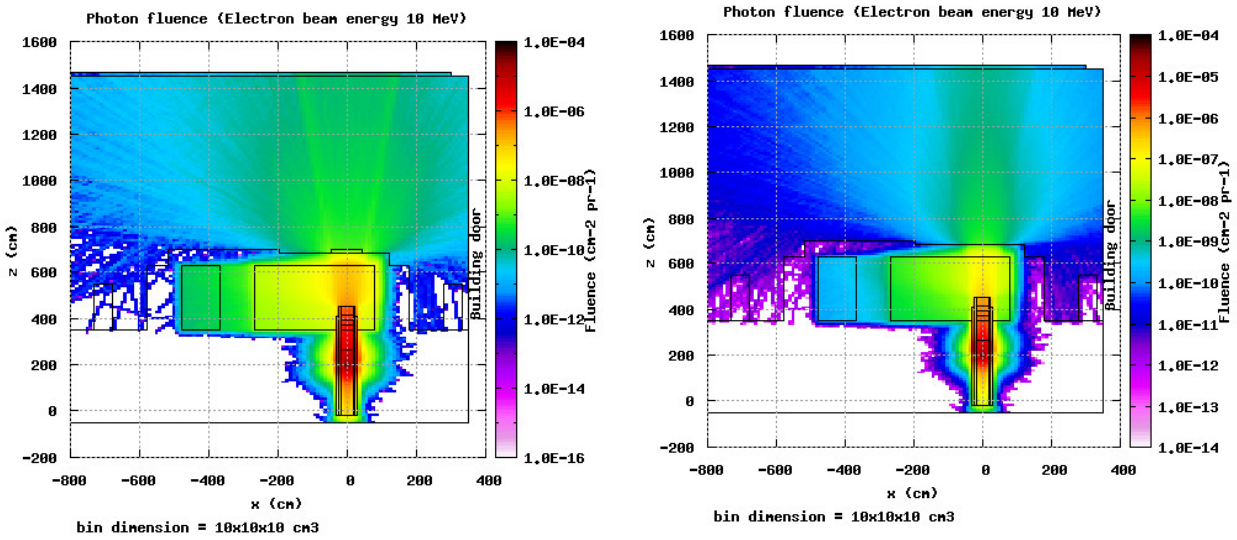

(a) (b)

Figure 22: View of the photon fluence with (a) and without (b) of the iron cylinder shield on the bunker roof

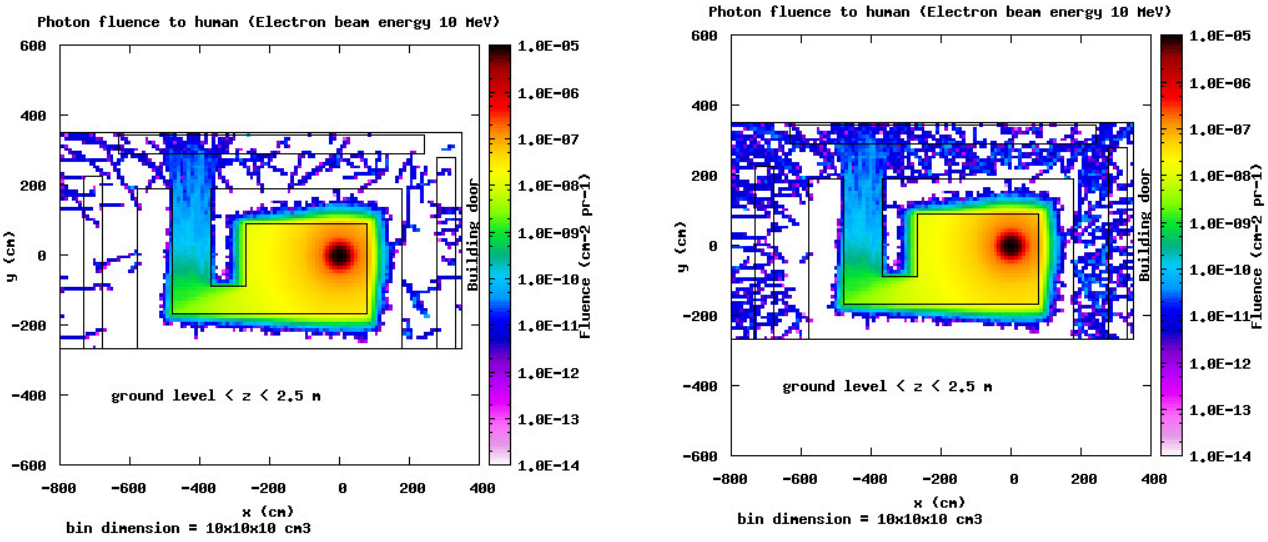

(a) (b)

Figure 23: Top view of the photon fluence between the floor level and 3 m (human window), with (a) and without (b) the iron cylinder shield over the concrete ceiling.

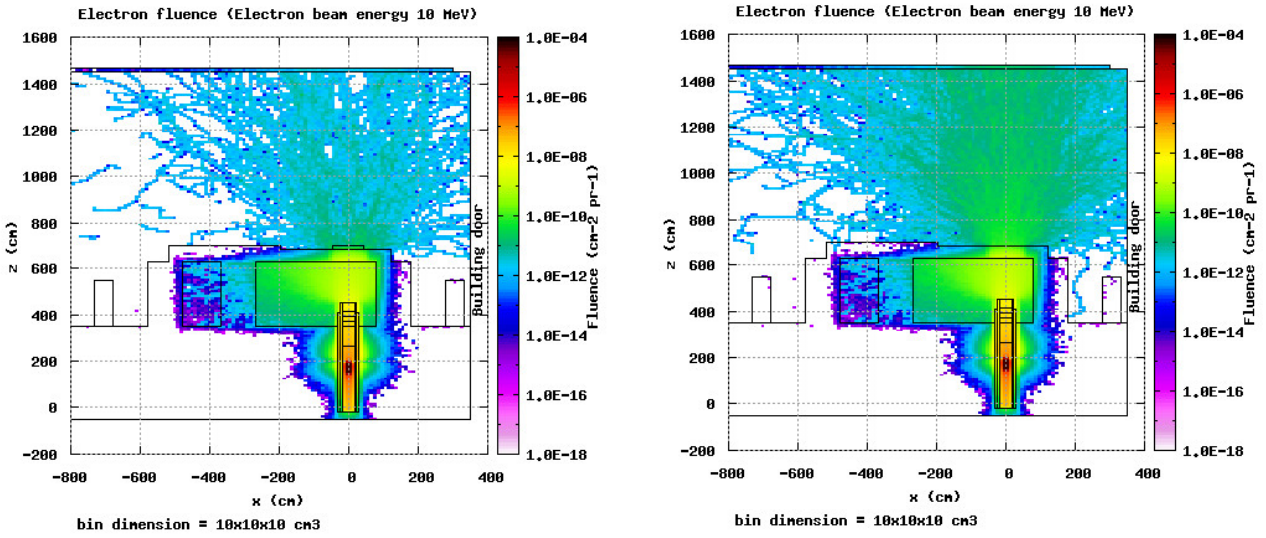

(a) (b)

Figure 24: View of the electron fluence with (a) and without (b) of the iron cylinder shield on the bunker ceiling.

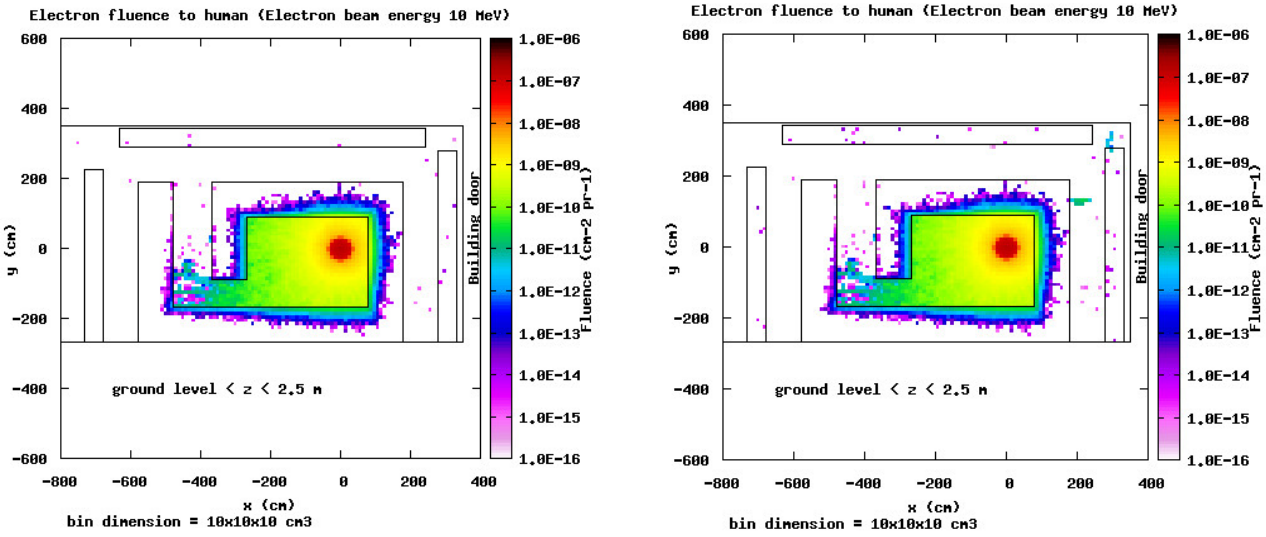

(a) (b)

Figure 25: Top view of the electron fluence between the floor level and 3 m (human window), with (a) and without (b) the iron cylinder shield over the concrete roof.

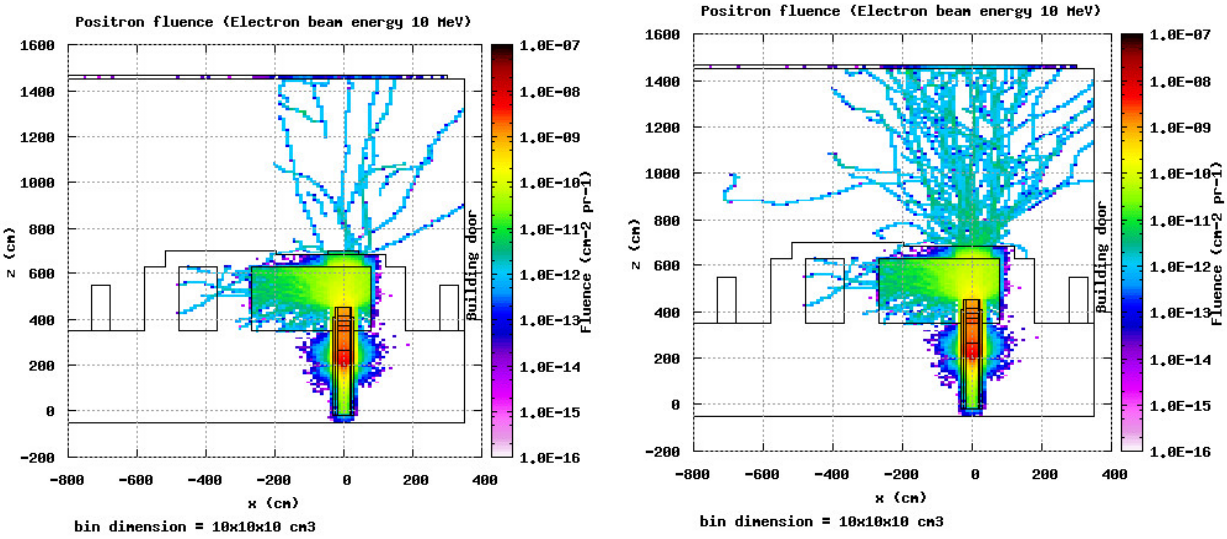

(a) (b)

Figure 26: View of the positron fluence with (a) and without (b) of the iron cylinder shield on the bunker roof

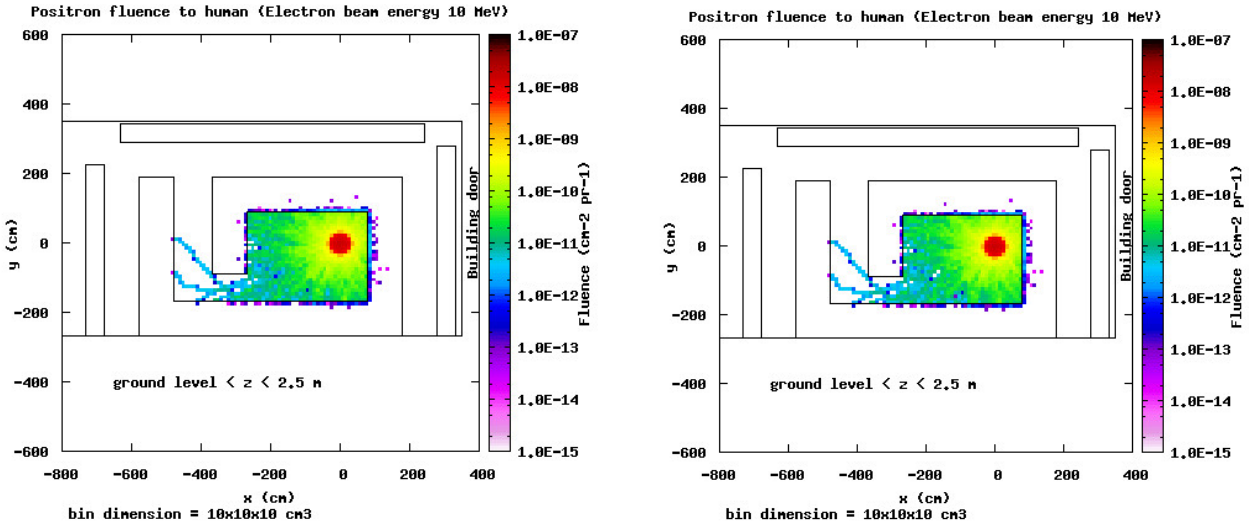

(a) (b)

Figure 27: Top view of the positron fluence between the floor level and 3 m (human window), with (a) and without (b) the iron cylinder shield over the concrete roof.

5.3 Fluencies toward the building door

The fluencies and spectra of the photons in the air just outside the walls of the bunker facing the building door - up to 3 m from them with and without the irons shield on the roof of the bunker - are shown in the following figures.

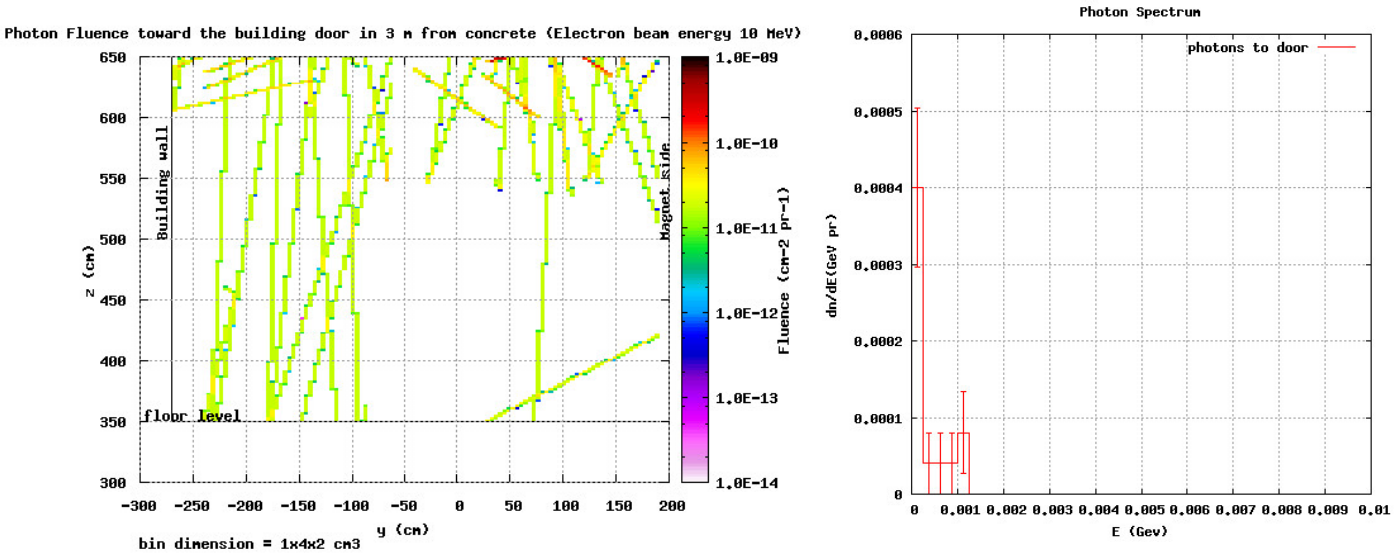

(a) (b)

Figure 28: (a) Photon fluence in 3 m outside the bunker wall toward the building door between ground level and 3 m height. (b) Spectrum of the photons exiting the bunker wall toward the building door, in the case with the iron shield on the bunker roof.

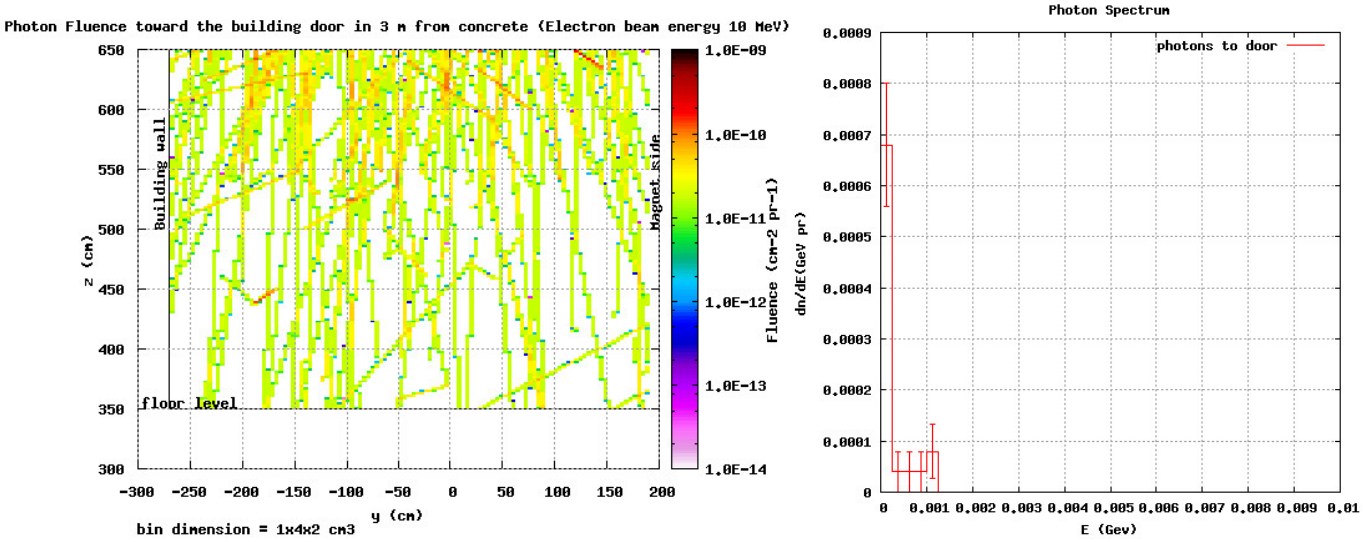

(a) (b)

Figure 29: (a) Photon fluence in 3 m outside the bunker wall toward the building door between ground level and 3 m height. (b) Spectrum of the photons exiting the bunker wall toward the building door, in the case without the iron shield on the bunker roof.

5.4 Fluencies toward the magnet area

In the following figure 30 and 31 the fluencies of the photons toward the magnet area with and without the irons shield are shown. The effect of the shielding is evident both on the fluencies and on the photon spectrum.

The electron and positron fluencies are negligible and both do not come directly from the concrete wall.

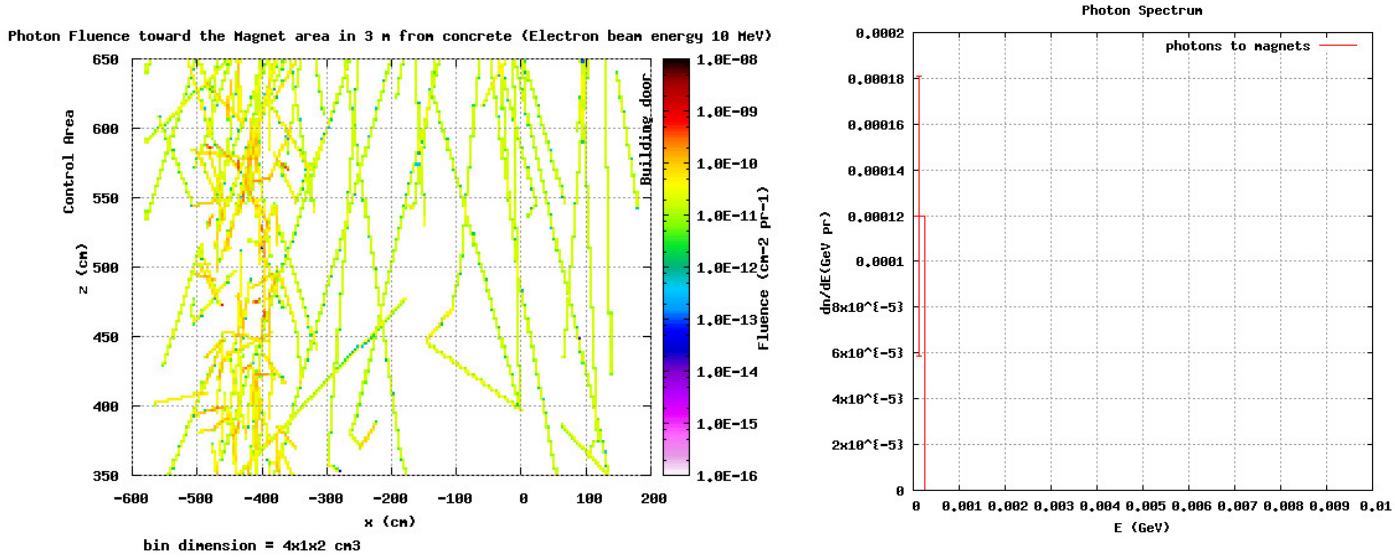

(a) (b)

Figure 30: (a) Photon fluence in 3 m outside the bunker wall toward the magnets between ground level and 2.5 m height. (b) Spectrum of the photons exiting the bunker wall toward the building door, in the case with the iron shield on the bunker roof.

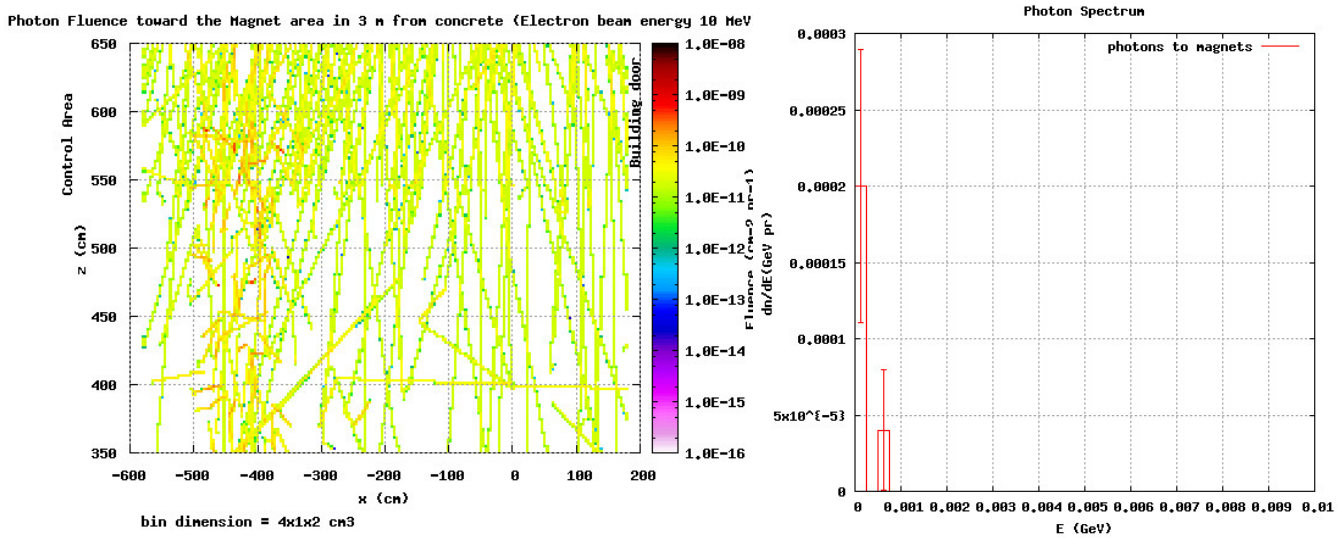

(a) (b)

Figure 31: (a) Photon fluence in 2.5 m outside the bunker wall toward the magnets between ground level and 2.5 m height. (b) Spectrum of the photons exiting the bunker wall toward the building door, in the case without the iron shield on the bunker roof.

5.5 Fluencies toward the control area

The fluencies of the photons toward the control area with (a) and without (b) the irons shield are shown In the following figure.

The effect of the shielding is evident. The electron and positron fluencies are negligible and both do not come directly from the concrete wall.

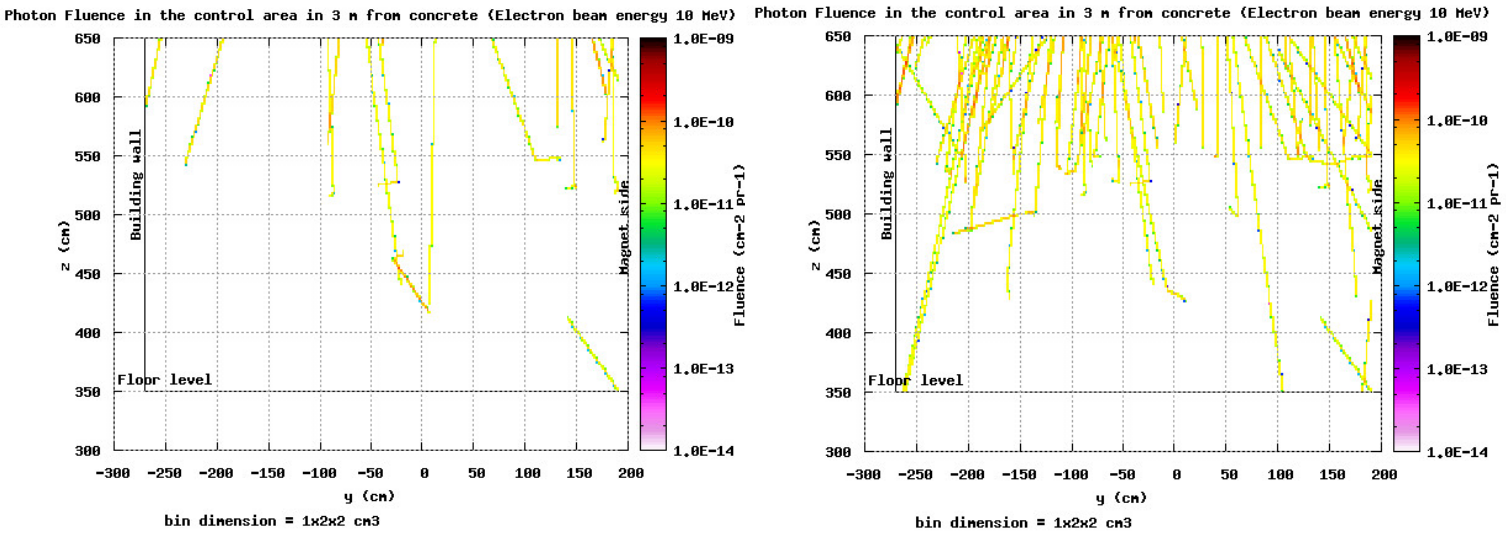

(a) (b)

Figure 32**:** (a) Photon fluence in 3 m outside the bunker wall toward the control area between ground level and 3 m height. With (a) and without (b) the iron shield on the bunker roof.

5.6 Detectors response

The detectors do not register any energy deposition, except the ones located on axis with the cryostat just over the bunker roof concrete and the detector inside the bunker at 1.83 m height respect to the floor level on axis with the cryostat.

The detector on axis inside the bunker is a cylinder with a radius of 2.54 cm, 20 cm height. The one just over the concrete ceiling of the bunker is a cube of 2x2x2 cm^3 volume.

A further refinement of the calculations was done by putting 4 further detectors, made of water, on the internal wall of the bunker, at 1.5 m from the floor level. They are located at the intersection between the green dotted line, facing the regions R14 and R12, and at the intersection of the blue dotted line, facing the regions R13 and R22 (see fig.18).

The dimensions were 2x2x2 cm^3. The case "With Iron" will be the normal operating condition, for this reason the data are more completed in this case.

The following table summarizes the energy and dose deposition in the detectors for the configuration with and without the iron over the bunker ceiling. The material column indicates whether the detector is present (water) or not (air), in this case the energy deposition in air in the volume of the detector is reported.

Table 2: Energy in the detectors.

	Without Iron				With Iron			
Detector	Material	Energy (GeV/pr)	Dose (Gy/h)	Error%	Material	Energy (GeV/pr)	Dose (Gy/h)	Error%
Inside the bunker	Water	3.35E-08	1.37E+00	2.82	Water	3.35E-08(*)	1.37E+00(*)	2.82(*)
Over the ceiling	Water	2.88E-11	6.23E-02	60.09	Water	=	=	=
Inside the bunker	Air	1.44E-11	5.88E-04	24.11	Air	1.34E-11	5.48E-04	23.98
Over the ceiling	Water	2.32E-10	5.01E-01	31.07	Water	=	=	=
Detector "A"					Water	1.20E-11	2.60E-02	58.75
Detector "B"					Water	2.98E-11	6.44E-02	38.46
Detector "C"					Water	1.87E-12	4.04E-03	61.57
Detector "D"					Water	1.10E-12	2.39E-03	99.0

The data reported in the case "With Iron" of the detector inside the bunker(*) are the same as the case without iron (it is not affected by the iron).

There is no energy deposition in the detector over the ceiling and iron when the iron is present.

The data of the energy deposition in the detector inside the bunker are very low with a large error so they can be considered as a statistical fluctuation, instead of an actual energy deposition.

6 CONCLUSIONS

The simulation of the field emission scenario of a superconducting radiofrequency cavity has been carried out by assuming an electron impact energy of 10 MeV, in its turn producing a radiation pattern with 10 MeV max energy. The results show that even in the theoretical limit case of $3x10^{13}$ electrons generated per second – corresponding to the maximum cryogenic load of 50W - the radiation level in all the critical points of the lab remains of the same order of background radiation (0.32 μSv/h). The maximum value, less than 1 μSv/m, is in the bunker door zone. The introduction of a further iron shield on the bunker roof significantly reduces the skyshine effect. Neutron production and materials nuclear activation are completely absent in the zones of interest.

By considering the ultra-conservative (and less probable) hypothesis (electron beam), and the less conservative (isotropic source) most likely the second one seems the most probable. As a matter of fact the first one requires the very improbable fact that the all dark current electrons will be in phase and accelerated by the cavity field, then gaining the maximum energy. Electron randomly emitted will see different RF phases and electric field, so the collimated monochromatic 10 MeV beam is a very remote possibility.

Anyway in the future, at the starting of the test in the upgraded configuration, experimental measurements of the dose around the bunker will be used to validate the shielding.

7 APPENDIX: SKYSHINE EFFECT

A preliminary run did not take into account the concrete building ceiling (11 m height), but the data shown so far indicate the skyshine effect (i.e. a backscattering from the building roof to the experimental area) is present.

In the following figures the fluencies of the photons, electron, and positrons obtained without the building ceiling (analogously to the plot of fig. 5, 6 and 7) are shown.

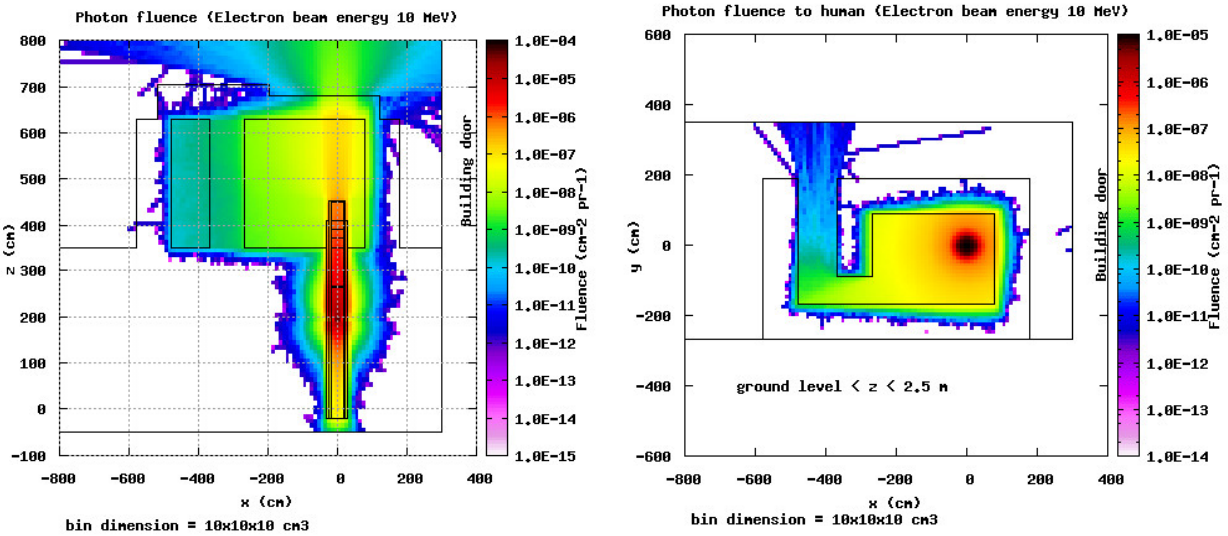

(a) (b)

Figure 33: (a) View of the photon fluence and (b) top view of the of the photon fluence between the floor level and 2.5 m (human window), without considering the building ceiling. To be compared with fig. 5, where the building ceiling is taken into account.

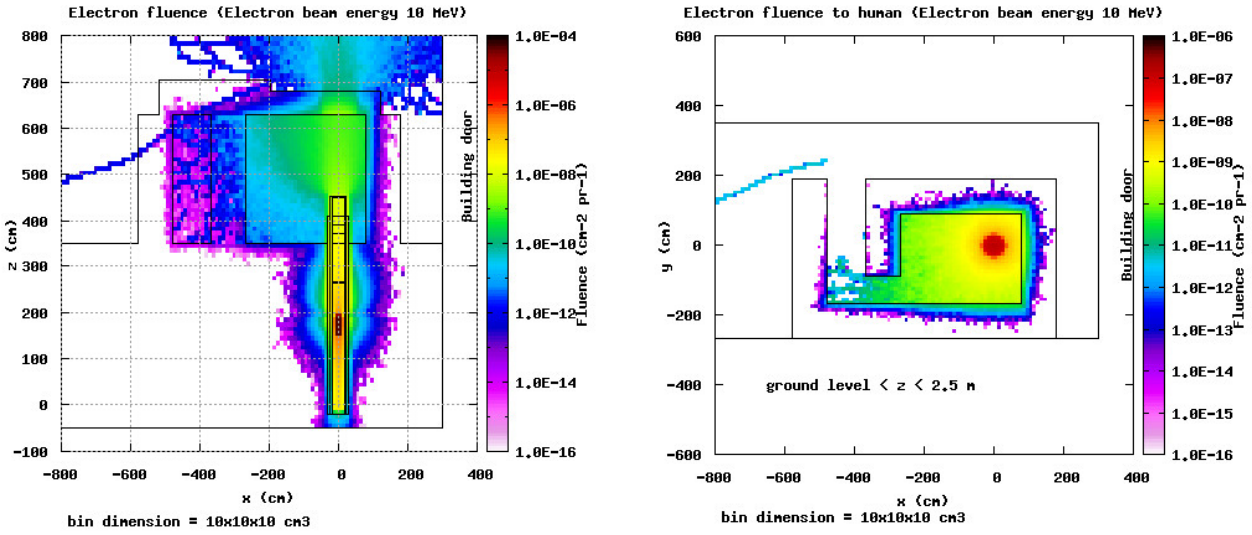

(a) (b)

Figure 34**:** (a) View of the electron fluence and (b) top view of the of the electron fluence between the floor level and 2.5 m (human window), without considering the building roof. To be compared with fig. 6, where the building roof is taken into account.

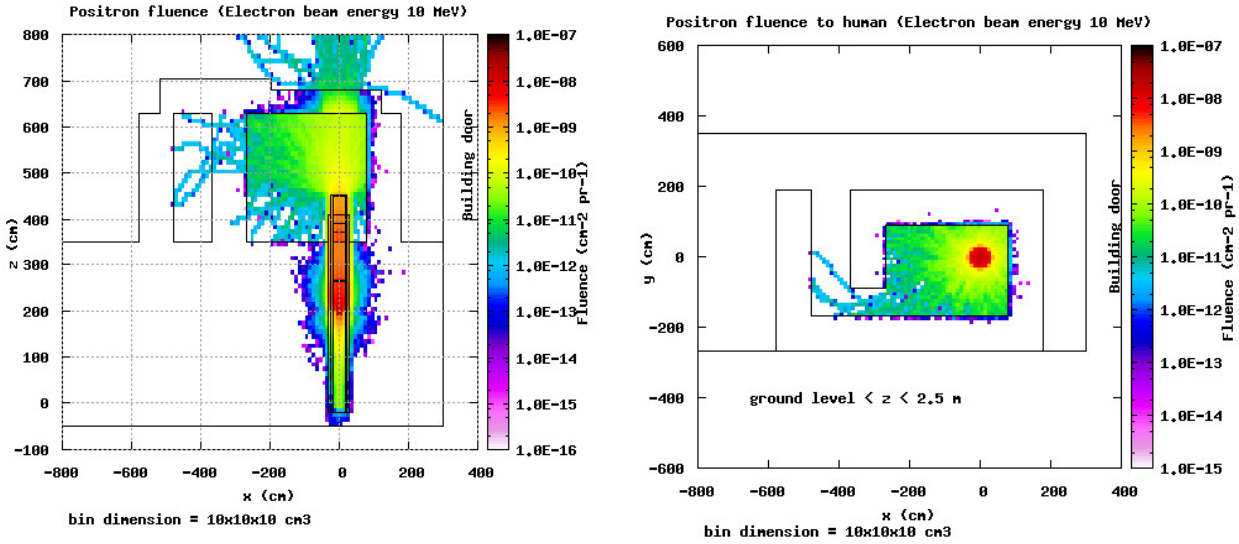

(a) (b)

Figure 35**:** (a) View of the positron fluence and (b) top view of the of the positron fluence between the floor level and 2.5 m (human window), without considering the building roof. To be compared with Fig. 7, where the building roof is taken into account.

8 REFERENCES

[1] P. Pierini, et al., “Fabrication and vertical test experience of the European X-ray Free Electron Laser 3.9 GHz superconducting cavities”, Phys. Rev. Accel. Beams 20, 042006 (2017)

[2] A. Bosotti et al., “Vertical Tests of ESS Medium Beta Prototype Cavities at LASA”, in Proc. 8th Int. Particle Accelerator Conf. (IPAC'17), Copenhagen, Denmark, May 2017, paper MOPVA063

[3] A. Ferrari, P.R. Sala, A. Fasso`, and J. Ranft, "FLUKA: a multi-particle transport code", CERN 2005-10 (2005), INFN/TC_05/11, SLAC-R-773

[4] T.T. Bohlen, F. Cerutti, M.P.W. Chin, A. Fasso`, A. Ferrari, P.G. Ortega, A. Mairani, P.R. Sala, G. Smirnov, and V. Vlachoudis, "The FLUKA Code: Developments and Challenges for High Energy and Medical Applications", Nuclear Data Sheets 120, 211-214 (2014)

[5] V. Vlachoudis, Proc. Int. Conf. on Mathematics, Computational Methods & Reactor Physics (M&C 2009),

[6] M. Santana Leitner, L. Ge, Z. Li, C. Xu, C. Adolphsen, M. Ross and M. Carrasco,” Studies of radiation fields of LCLS-II super conducting radio frequency cavities”, Applications of Nuclear Techniques (CRETE15), International Journal of Modern Physics: Conference Series Vol. 44 (2016) 1660209.